Proceedings of ISFOG 2025
5TH INTERNATIONAL SYMPOSIUM ON
FRONTIERS IN OFFSHORE GEOTECHNICS
Nantes, France | June 9-13 2025

ISBN 978-2-85782-758-0

Detailed parametric monopile-spudcan interaction assessment in clay and sand dominated soil stratigraphies

J.A. Rebollo Parada*
Geowynd Ltd., London, United Kingdom

L. Zuccarino
Geowynd, Milano, Italy

P. Hu
Western Sydney University, Sydney, Australia

L. Jones
Independent Consultant, London, United Kingdom

D. Rushton
East Point Geo, Norwich, United Kingdom

**jur@geowynd.com*

ABSTRACT: This article presents a detailed parametric assessment of monopile-spudcan interactions for two WTG locations embedded in predominantly clay and sand soil profiles. The analysis follows a two-stage coupled approach. The first stage makes use of Large Deformation Finite Element Analysis (LDFEA) to model the spudcan penetration and extraction, assessing the extent and magnitude of the disturbance in the surrounding soil volume as well as the residual seabed footprint following extraction. In the second stage, a parametric monopile-spudcan interaction analysis is conducted using 3D finite element analysis (FEA) simulations. The effects of the spudcan installation and extraction on the surrounding soil are represented by modelling the spudcan crater and modifying the soil properties of the disturbed soil volume to reflect the expected soil remoulding. The 3D FEA includes representative cyclic soil degradation in storm conditions to allow the verification of the monopile lateral capacity under extreme storm loads. The results with and without spudcan disturbance are then compared to assess the relative loss in capacity and stiffness. A parametric analysis with multiple monopile-spudcan offsets and spudcan penetration depths is performed to identify a safe distance between the monopile and spudcan footprint for each geotechnical soil profile, based on an acceptable reduction in ultimate capacity with respect to the base case.

Keywords: Offshore, spudcan, monopile, FEM, LDFEM

1 INTRODUCTION

Jack-up vessels are frequently used to install monopile foundations and wind turbine generators (WTGs) at offshore wind farm sites. The installation and removal of jack-up spudcan foundations causes significant deformations in the surrounding soil and creates a residual seabed footprint. These residual effects can interact with the WTG foundation during its operational life. Therefore, geotechnical designers must investigate the effects of monopile-spudcan interaction, considering spudcan geometry, offset to the foundation, and soil conditions.

This article presents a detailed parametric assessment of monopile-spudcan interactions for two 15MW WTG locations in approximately 50 m water depth embedded in predominantly clay and sand soil profiles, representing typical North Sea soil conditions, to identify a safe distance between the monopile and spudcan footprint for each geotechnical soil profile, based on acceptable capacity loss under cyclic storm loading.

While some general recommendations for spudcan-foundation interaction exist in the literature, like the ABS recommendations in homogeneous clay soil (American Bureau of Shipping, 2018), it is uncertain if these can be applicable to the layered profiles found in sites targeted by the offshore wind industry. This paper proposes an= finite element analysis (FEA)-based approach to determine both the extent of the spudcan footprint and the interaction with the neighbouring monopile foundation.

To evaluate the extent of the residual spudcan footprint and the degree of degradation on the surrounding soil volume, a free-field large-deformation finite element analysis (LDFEA) has been performed. The LDFEA was used to model the

installation and removal of the spudcan, and the evolution of plastic shear strains during the process.

Based on the residual strain field, the extent of the footprint and degraded soil volume have been defined. These have been modelled alongside the wished-in-place monopile foundation in a 3D FEA model, and subjected to the design load set. Finally, a parametric analysis has been performed at multiple edge-to-edge monopile-spudcan distances to assess the impact of the spudcan on foundation ultimate capacity.

2 SOIL CONDITIONS

Two layered soil profiles have been used for this analysis, based on site data from two locations in the North Sea. The locations present typical conditions, namely:

- Location 1: Soft clay over dense sand.
- Location 2: Loose sand over stiff clay.

The main soil parameters for each location are presented in

Table 1 and

Table 2, namely the unit weight (γ), undrained shear strength (s_u), sensitivity (S_t), over-consolidation ratio (OCR), relative density (D_r), internal friction angle (φ), dilatancy angle (Ψ) and interface friction angle (δ). In addition, each location included CPT data as well as basic and advanced cyclic laboratory testing used to define the cyclic properties and backbone curves of each soil layer.

3 FREE-FIELD LDFE ANALYSIS

3.1 Analysis setup

The 3D LDFEA was conducted simulating the spudcan as a rigid body penetrating vertically through the soil profile to the termination depth, before moving vertically upwards returning to zero penetration depth. Taking advantage of the radial symmetry of the problem, a quarter of the model was simulated.

The behaviour of clay was modelled using the modified Tresca model, which incorporates a strain-softening behavior introducing a gradual reduction in shear strength with increasing plastic shear strain. The sand was described using a modified Mohr-Coulomb constitutive model. The model allows the internal friction angle and dilation angle to vary with accumulated plastic shear strain.

Table 1: Location 1 soil profile

Depth $[m]$		**Soil type**	$\gamma\left[\frac{kN}{m^3}\right]$	s_u $[kPa]$	S_t $[-]$	OCR $[-]$	D_r [%]	φ [°]	Ψ [°]	δ [°]
Top	**Bottom**									
0.0	1.5	Clay	19.1	12	1.4	16				
1.5	4.0	Clay	19.1	23	1.4	6.5				
4.0	7.0	Clay	19.1	15	1.4	2				
7.0	10.0	Clay	19.1	17	1.4	1.4				
10.0	12.9	Clay	19.1	22	1.4	1.3				
12.9	13.6	Sand	20.2				46	34	0.8	29
13.6	16.1	Sand	20.1				58	34	4.5	30
16.1	17.4	Sand	20.2				30	33	1.7	29
17.4	20.0	Sand	20.1				83	38	0.3	30
20.0	26.5	Sand	20.2				82	38	1.8	29
26.5	29.4	Clay	21.9	800	1.2					

Table 2: Location 2 soil profile

Depth $[m]$		**Soil type**	$\gamma\left[\frac{kN}{m^3}\right]$	s_u $[kPa]$	S_t $[-]$	OCR $[-]$	D_r [%]	φ [°]	Ψ [°]	δ [°]
Top	**Bottom**									
0.0	0.8	Sand	20.2				20	33	0.1	29
0.8	6.8	Sand	20.1				62	35	2.4	30
6.8	8.3	Clay	21.0	37	1.3	2				
8.3	10.3	Clay	21.9	691	1.2	13				
10.3	13.7	Clay	21.9	950	1.2	13				
13.7	17.6	Clay	21.9	1824	1.2	13				
17.6	21.6	Clay	21.9	1808	1.2	13				
21.6	24.6	Clay	21.0	301	1.3	3.5				
24.6	26.7	Clay	21.9	516	1.2	3.5				
26.7	30.0	Clay	21.9	611	1.2	3.5				

The modified Mohr-Coulomb model assumes that the friction angle increases linearly from an initial value to the peak value φ_{peak} before decreasing linearly to the critical-state friction angle φ_{cv} as the material reaches the critical state. More details of both models can be found in Hu et al. (2015). The numerical simulations were carried out using commercial software Abaqus (Dassault Systèmes, 2018). The spudcan and the stratified soils were discretised using Lagrangian and Eulerian meshes, respectively. The mesh is shown in Figure 1.

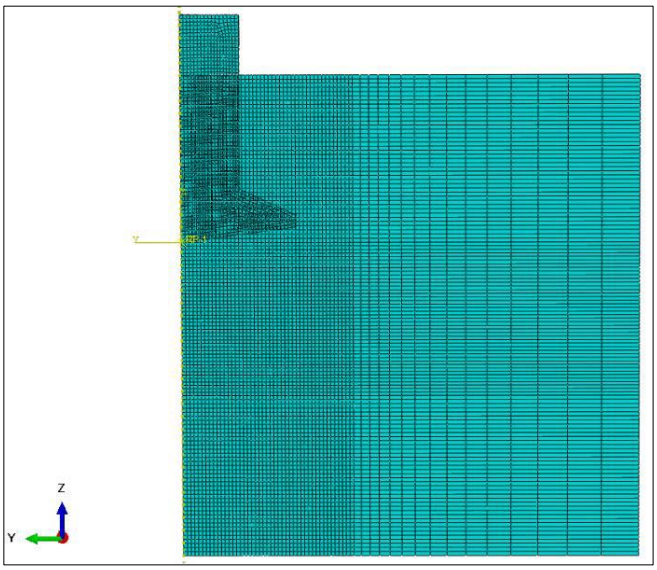

Figure 1: Front view of free-field 3D LDFEA mesh for Location 1.

A finer mesh zone was set along the penetration-extraction trajectory of the spudcan, refining the soil region in contact with the spudcan to enhance the accuracy of the simulation.

3.2 Spudcan geometry and boundary conditions

The spudcan is assumed to have a circular footprint section, with an equivalent diameter of 19.2m and a bearing area of 290 m^2. The simplified side section considered for this paper is shown in Figure 2.

The spudcan was installed using a displacement-controlled boundary condition until a prescribed penetration depth of 14.0 m for Location 1 and 9.0 m for Location 2, consistent with predicted penetrations.

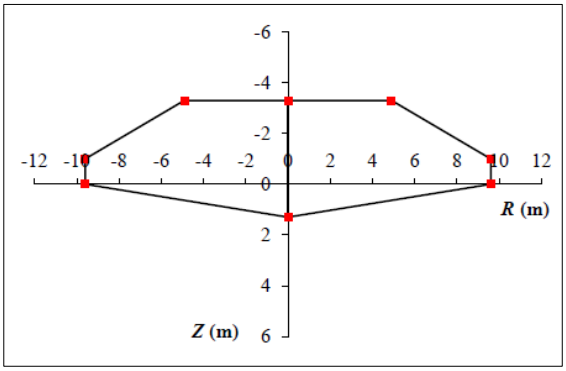

Figure 2: Simplified spudcan geometry.

3.3 Results

During the spudcan penetration process, a significant volume of soil is mobilised and remoulded. The soil below the spudcan gets squeezed downwards and sidewards, mobilising a large volume of surrounding soil. As the penetration continues, the cavity above the spudcan top is filled by the remoulded soil mixture. In Location 1, the top five clay layers predominantly deform laterally, indicating a squeezing failure mechanism where the softer clay is displaced outward rather than downward. The sand layers below show minimal deformation, indicating that they act as a relatively rigid base, restricting downward movement and forcing the clay layers to deform laterally.

This behaviour is consistent with the low stiffness and high compressibility of the clay layers relative to the underlying sand, leading to pronounced lateral extrusion. During extraction, the clay above the spudcan was displaced sideways, but no backflow occurred to fill the cavity due to the strength and cohesion of the upper clay layers. For Location 2, there is minimal deformation in the deeper clay layer starting from 8.3 m depth, confirming that it acts as a stiff barrier, preventing downward deformation and causing the overlying layers to squeeze out laterally. The upper layers, including both clay and sand, undergo significant lateral deformation, further reinforcing the squeezing failure mechanism as the dominant mode of deformation. Notably, the sand layers do not form a sand plug, possibly due to low ratio of sand layer thickness and spudcan diameter. During the spudcan extraction, this soil mixture gets pushed upwards onto the surface, generating a berm on top of the surrounding seabed. Once the spudcan clears the seabed level, this berm tends to collapse onto the crater, forming a residual conical footprint. This evolution is shown in Figure 3 and Figure 4.

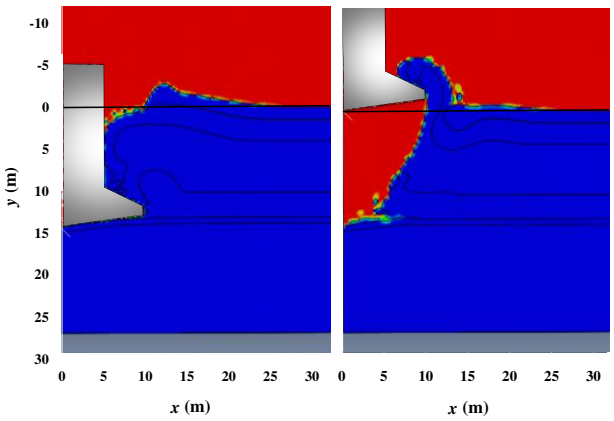

Figure 3: Deformed soil profile at the end of the spudcan penetration (left) and extraction (right) at Location 1.

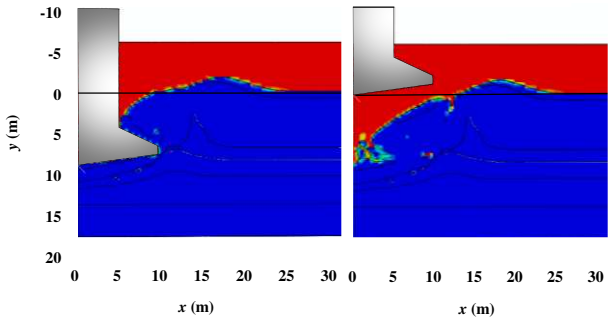

Figure 4: Deformed soil profile at the end of the spudcan penetration (left) and extraction (right) at Location 2.

The extent of the degraded soil zone can be examined from review of the plastic shear strain contours. The degraded soil zone geometry has been established by using a 10 % plastic shear strain contour as a threshold limit. This is considered a conservative estimate of the shear strain required to fully remould the soil volume.

The resulting remoulded soil geometry, as shown in Figure 5, is an input for the 3D FE analysis described in the following sections. Specifically in Location 1, dominated by soft clays, the remoulded zone inferred from the LDFEA has been compared to the ABS recommendations for soft to firm clay. ABS proposes a normalized graph to assess the extent of the soil degradation depending on the spudan footprint and penetration depth differenciating between heavily, moderately and less disturbed zones. It can be appreciated that the boundaries of the LDFEA remoulded zone are generally in good agreement with the ABS boundaries, falling around the 'moderately disturbed' line up until the start of the sand layer, where the LDFE solution results in a shallower remoulded zone. This is expected, given that the ABS recommendation is meant for homogeneous clay profiles.

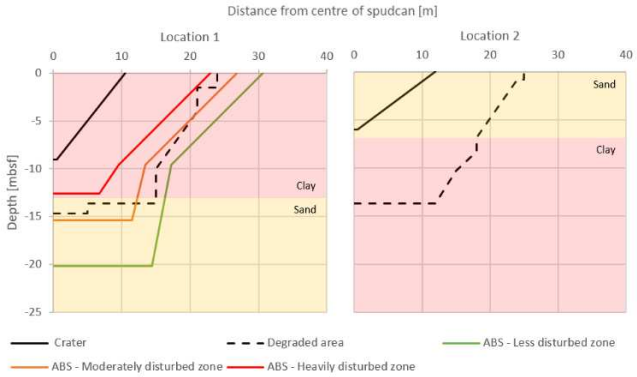

Figure 5: Degraded soil geometry of Location 1 (left) and Location 2 (right)

The displacements induced by spudcan installation and extraction are also of interest when considering interaction with other seafloor assets, such as scour protection systems or electrical cables. To assess the induced soil movements, displacements were extracted from the LDFEA at four horizontal distances from spudcan edge and for three depths below seabed. The spudcan installation/extraction induced maximum total displacements for each selected point are provided in Table 3.

Table 3: Spudcan installation/extraction induced maximum total displacements

Location	**Depth [m]**	**Maximum total displacement at specified horizontal distance from spudcan edge [m]**			
		4.8	10.0	14.2	25.6
1	0.0	1.89	0.89	0.14	0.01
	1.5	1.78	0.65	0.04	0.01
	3.0	1.68	0.40	0.03	0.01
2	0.0	1.35	1.60	0.14	0.00
	1.5	2.34	0.97	0.02	0.00
	3.0	2.69	0.45	0.01	0.00

The extent of the seabed disturbance in both locations is quite similar, dissipating at approximately 15m around the spudcan edge. However, maximum displacements at Location 2 occur farther away from the spudcan compared to Location 1. This result is in agreement with the expectation of a wider, spread-out passive wedge in the sand-dominated profile compared to a more local failure mechanism in the clay-dominated location. This behaviour is also reflected in Figure 3 and Figure 4.

4 MONOPILE-SPUDCAN INTERACTION ANALYSIS

4.1 Analysis setup

The 3D FE analyses were performed using the commercial software Plaxis 3D V21 (Bentley, 2021).

The 3D FEA mesh of the soil was developed using ten-noded quadratic fully integrated tetrahedral elements. The FE model comprised half of the pile and soil, considering the symmetry of the laterally loaded monopile problem. All vertical boundaries, including the plane of symmetry, were normally fixed, and the lower horizontal boundary was fully fixed. Six-noded triangular shell elements were used to model the steel pile wall. The pile steel was represented using a linear elastic model with a Young's modulus (E) of 210 GPa and a Poisson's ratio (v) of 0.3. Between the pile wall and the soil, twelve-noded interface elements are used to model the soil-structure interaction.

The monopile was subjected to a lateral load-controlled procedure until the lateral displacement at seabed reached 10% of the monopile diameter, which was the failure criterion set for the present study. To represent the storm loading conditions of the site at seabed level, a moment-to-shear ratio of 60 was used. A so-called staged construction approach was performed, with the main calculation stages of the FEA listed below:

- Stage 1: Initial or geo-stresses stage; where the initial stresses from the soil volume are simulated using a K_0 procedure.
- Stage 2: Installation; where the foundation and the associated interfaces are activated in the model. The field stress distribution is updated due to the presence of the monopile inside the soil volume.
- Stage 3: Horizontal load; where the monopile foundation is subjected to the considered horizontal shear force and overturning moment.

The effects of the cyclic loading from the Ultimate Limit State (ULS) storm event, in terms of the pore pressure build-up and the accumulated shear strains, were taken into account within the cyclic degradation model used for the analysis. The analysis employed the Parallel Iwan Multi-Surface (PIMS) constitutive soil model (Whyte et al., 2020) for both sand and clay, calibrated against cyclic backbone stress-strain curves measured from site-specific laboratory test data. Location-specific cyclic degradation assessments were performed at each soil layer, following the methodology outlined by (Andersen, 2015).

To include the effect of spudcan penetration and extraction, a degraded soil volume and spudcan footprint in the seabed (crater) were introduced to the base case (i.e. monopile-only) 3DFEA model. A schematic representation of the spudcan interaction 3DFEA model is shown in Figure 6.

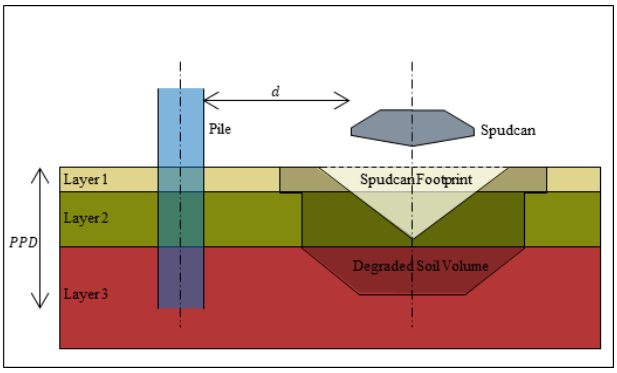

Figure 6: 3DFEA monopile-spudcan interaction model

To represent the development of the large deformation plastic strain field around the spudcan, a degraded soil volume was introduced in the model. The extent of the remoulded zone was based on the LDFEA results, as discussed in Section 3.3.

The soil inside the selected remoulded volume has been modelled with degraded properties, while the rest of the soil volume uses the original cyclic properties. To model the large deformation effects in sand, it was assumed that the material would undergo a densification and stress relaxation and tend to the critical-state relative density. In practice, this was modelled by degrading the reference stress in the PIMS cyclic backbone curves by a factor of 0.7. In clays, to model the fully remoulded properties, the undegraded cyclic backbone stress was divided by the clay sensitivity.

The soil crater following spudcan extraction was represented by a removal of the soil volume estimated based on the LDFEA results. For simplicity, the crater was modelled as a single conical slope reaching the original seabed, assuming any residue left above the original level is scoured away.

A mesh density of approximately ~60,000 elements was considered. An example of the model mesh is shown in Figure 7. The element distribution across the mesh was optimised to provide local refinement in the zones close to the pile shaft and tip, while limiting the number of elements in the outer zones of the model.

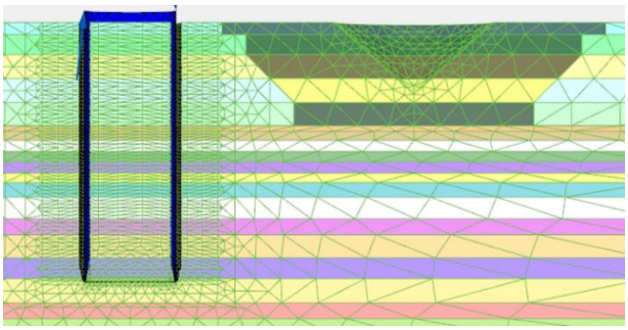

Figure 7: Detail of the front view of 3DFE mesh for Location 1.

4.2 Monopile geometry

The monopile geometries are presented in Table 4.

Table 4. Monopile geometry

Location	Outer Diameter [m]	Wall Thickness [mm]	Pile Penetration [m]
1	11.50	78.00	33.75
2	11.50	78.00	25.50

4.3 Parametric analysis

For each location, a set of 3D FE analyses was run by incrementing the monopile edge to spudcan edge distance (d in Figure 6) from 10 m to 25 m in steps of 5 m, or until a negligible effect on the foundation capacity was found. These analyses are compared with a 'base case' scenario with no spudcan interaction.

For each case, the lateral force-displacement curve at seabed was extracted, obtaining the acting force at a horizontal displacement equal to 10% of the monopile diameter. Comparing the lateral force of each interaction case with the base case, a performance based utilisation ratio $UR_{0.1D}$ can be derived:

$$UR_{0.1D} = \frac{F_{x,i}}{F_{x,0}} \quad (1)$$

Where:

- $F_{x,i}$ is the monopile-acting lateral force, for a given spudcan interaction offset i, when the seafloor displacement equals 10% of pile diameter.
- $F_{x,0}$ is the monopile-acting lateral force, for the base case (i.e. no spudcan interaction effect), when the seafloor displacement equals 10% of pile diameter.

The resulting $UR_{0.1D}$ are presented in Table 5. The effect of spudcan interaction is found greater for Location 1 and increases as the monopile-spudcan offset decreases.

Table 5: Utilisation ratios

Location	Monopile-spudcan offset [m]			
	10.0	15.0	20.0	25.0
1	0.963	0.978	0.987	0.993
2	0.988	0.994	0.997	-

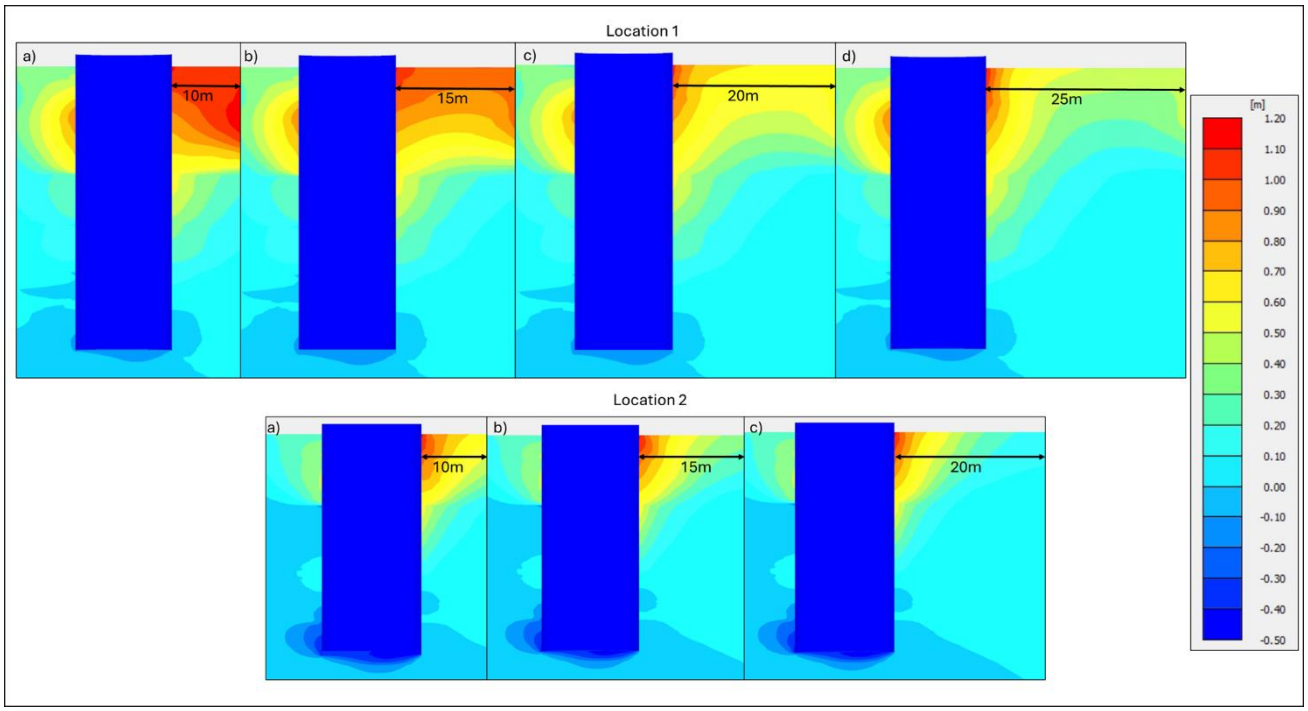

Figure 8: Displacement contours for different monopile-spudcan offsets - a) d=10m, b) d=15m d, c) d=15m and d) 20m

5 RESULTS AND CONCLUSIONS

The current work establishes a methodology to determine the impact of the penetration and extraction of a spudcan on the ULS in-place capacity of a monopile foundation under cyclic storm conditions.

The objective of this parametric analysis is to define a 'safe' monopile-spudcan edge-to-edge distance at which a negligible reduction in foundation lateral capacity is expected for different scenarios. The definition of a 'negligible' loss in capacity in the case presented in this paper was set as 1%, i.e. UR of 0.99.

As per the results in Table 5, this criterion implies an offset of at least 25 m for Location 1 and 15 m for Location 2. This shows that the impact of the monopile-spudcan offset on the interaction effects can be strongly dependent on the specific soil stratigraphy.

In addition, it can be expected that the jack-up operation may disturb the existing seabed in a very wide area around the spudcan, independently of the soil conditions. This should be taken into account when planning the installation of other superficial elements such as the scour protection or the cable protection system.

AUTHOR CONTRIBUTION STATEMENT

Juan Rebollo: Methodology, FE Analysis, Writing. **Lorenzo Zuccarino**: Methodology, Supervision, Reviewing. **Pan Hu**: LDFE Analysis, Writing. **Lewis Jones**: Conceptualisation, Reviewing. **David Rushton**: Reviewing

REFERENCES

American Bureau of Shipping (2018). Guidance Notes on Geotechnical Performance of Spudcan Foundations, Houston, USA.

Andersen, K. (2015). Cyclic soil parameters for offshore foundation design. In: 3rd ISSMGE McClelland Lecture. Frontiers in Offshore Geotechnics III, Oslo, Norway, Volume 1, pp. 5–82.

Bentley (2021). Plaxis 3D Ultimate V21. Available at: https://www.bentley.com/software/plaxis-3d/

Dassault Systèmes (2018). Abaqus analysis users' manual. Providence, RI, USA: Simulia Corp.

Hu, P., Wang, D., Stanier, S. A., and Cassidy, M. J. (2015). Assessing the punch-through hazard of a spudcan on sand overlying clay. Géotechnique, 65(11), 883-896.

Whyte, S. A., Burd, H. J., Martin, C. M., Rattley, M. J. (2020) Formulation and implementation of a practical multi-surface soil plasticity model, *Computers and Geotechnics*, vol. 117, https://doi.org/10.1016/j.compgeo.2019.05.007